Effect of coil to tubular workpiece magnetic coupling on electromagnetic expansion process

S. K. Dond[1*], Tanmay Kolge [2], Hitesh Choudhary [2], Archana Sharma[2]

[1] Homi Bhabha National Institute, Maharashtra, India
[2] Bhabha Atomic Research Centre, Maharashtra, India
* Corresponding author. Email: shandond12@gmail.com

Abstract

Efficiency of the electromagnetic forming process is very less. Leakage flux contributes to a fraction of total energy loss in the forming process, and it is related to the coupling between the coil and workpiece. The workpiece experiencing Lorentz force should be as close as possible to the tool coil in order to achieve higher utilization of discharge energy. In this paper, experimental and numerical simulation study is performed to observe the coil-tube magnetic coupling effect on tube expansion and thereby on process efficiency. Aluminum tube of 100 mm length and 1.5 mm thickness is electromagnetically expanded using a 7 turn helical coil. Trials are taken for the different gaps between the coil and tube whereas discharge energy kept constant. 2D sequentially coupled numerical simulation carried out using COMSOL software. The tube displacement and the coupling factor obtained in the simulation showed good agreement with experimental observations. The coupling factor decreases with increase in the coil-tube gap. The Process efficiency and tube displacement are found to be improved exponentially with increasing in coupling factor. Considering various design aspects, coil and workpiece should be tightly coupled to achieve higher process efficiency.

Keywords

Energy efficiency, Metal forming, Simulation

1 Introduction

Electromagnetic forming (EMF) technology has attracted aerospace and automobile industries because of its advantages over conventional forming and welding methods (Golovashchenko, 2006). The typical EMF system is shown in Fig. 1 consist of the capacitor bank, power supply, discharge switch and tool coil with workpiece. Stored energy in capacitor bank is discharged and under damped current flows in the tool coil. Eddy current generates in the workpiece because of time varying magnetic field produced by the coil.

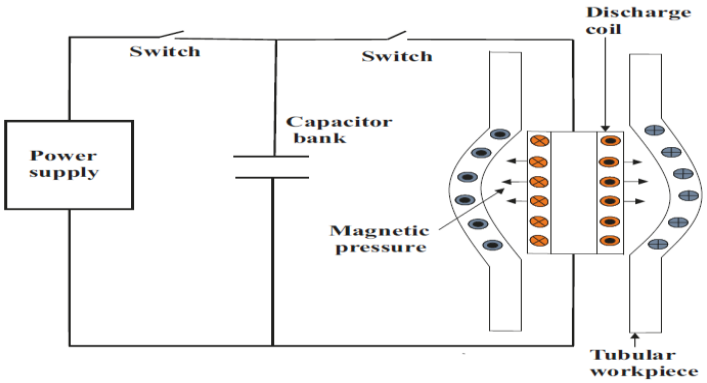

Figure 1: *Schematic of EMF system*

The interaction of the magnetic field between coil and workpiece results in repulsive force which is used to deform the workpiece. In EMF, electrical efficiency describes the transfer of electrostatic energy stored in capacitor banks to the electromagnetic energy in the tool coil whereas mechanical efficiency is the ratio of electromagnetic energy to forming energy. The overall process efficiency in electromagnetic forming applications is very less (Psyk et al., 2011, Haiping and Chunfeng, 2009). One of the factor causing less efficiency is the leakage flux and that is relevant the coil and workpiece magnetic coupling. The magnetic field coupling alters the discharge circuit parameters. Author, Xu et al. (2008) observed that the discharge circuit inductance exponentially increases and the resistance exponentially decays with the increase in distance between the coil and the workpiece.
In this paper, experimental and numerical study is performed to obtain magnetic coupling factor variation with coil-workpiece gap. A 2D axisymmetric numerical model is developed in COMSOL multiphysics. Electromagnetic expansion is carried out for different diameter aluminum tubes keeping the discharge energy and tube thickness constant. Numerical model results are compared with experimental ones and the model further used to study the effect of coil-tube coupling on the tube forming and process efficiency.

2 Electrical equivalent circuit

The Electrical equivalent circuit of EMF is shown in Fig.2. R_c and L_c are the coil resistance and inductance whereas R_w and L_w are tubular workpiece resistance and inductance respectively. System resistance R_s and inductance L_s is obtained from the current waveform of system short circuit test.

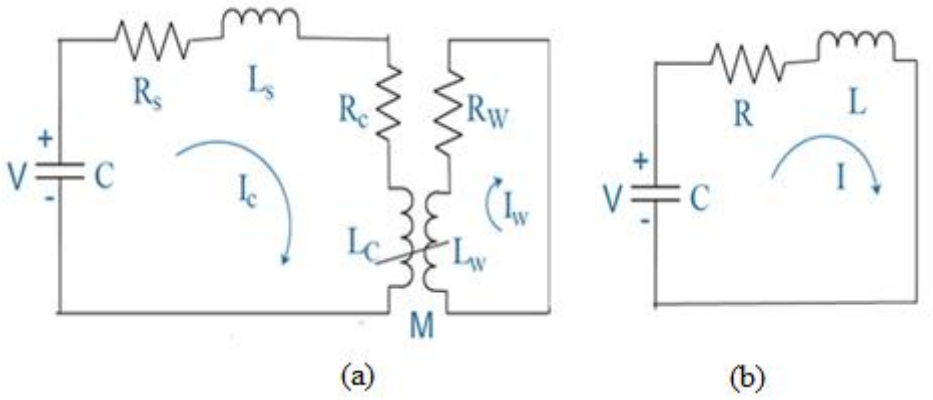

Figure 2: *Electrical equivalent circuit of EMF (a) exact version (b) reduced version*

The coupling between coil-workpiece can be compared to the transformer primary - secondary winding coupling, Aluminum tube can be assumed as a short circuited single turn secondary coil. The tube is mutually coupled to the discharge coil. Total equivalent inductance L and resistance R of coupled system can be written in following form (Mamalis et al., 2004, Zapata and Bay, 2016).

$$L = L_s + L_c - \frac{M^2}{L_w} \tag{1}$$

$$R = R_s + R_c + \frac{M^2}{L_w^2} R_w \tag{2}$$

$$M = K\sqrt{L_C L_w} \tag{3}$$

Here M is coil-tube mutual inductance. K is the coupling factor between coil and workpiece. K varies between 0 for uncoupled to 1 for the fully coupled system. Coupling factor decreases with increase in coil-workpiece gap. Thus resultant value of L increases and resistance R decreases with decrease in coupling factor.

$$i(t) = \frac{V}{\omega L} e^{-\beta t} \sin(\omega t) \tag{4}$$

$$\beta = \frac{R}{2L} \tag{5}$$

$$\omega = \sqrt{\frac{1}{LC} - \beta^2} \quad (6)$$

The discharge current flowing through the coil is given by Eq. 4, where V is the charging voltage of the capacitor, β is the damping coefficient and ω is the angular frequency of discharge current. Change in coupling affects the value of R and L in the above equation thus changing the β and ω value.

Experimental procedure

A 7 turn helical coil is used in the experiment. Arrangement and dimensions are shown in Fig. 3. All the experiments are carried out at constant discharge energy keeping charging voltage to 13.6 kV and capacitance 112 µF. The experimental set up is as shown in Fig. 4.

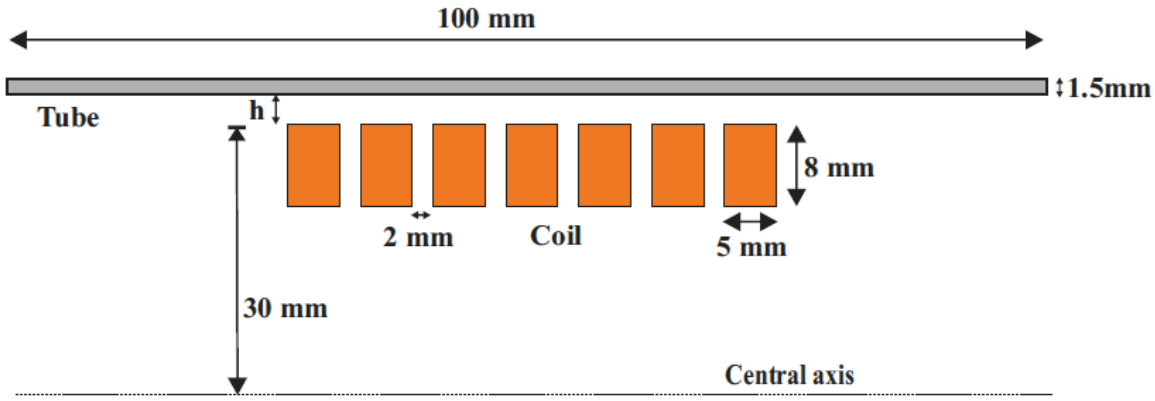

Figure 3: *Arrangement of coil, aluminum tube with dimensions*

Aluminum tube is placed over the discharge coil and the coil ends are connected to high current discharge terminals. Uniform gap between the coil and tube along the axial direction is maintained by a supporting structure made up of delrin. Discharge current is measured using Rogowaski coil. Different experiments are performed with increasing the coil-tube gap by 1 mm. Coil-tube coupled inductance L_{cw} is given by Eq. 7. A tube is placed over the coil, and inductance L_{cw} is measured at the coil terminals using an LCR meter. The coupling factor K can be obtained using Eq. 3 and Eq. 7.

$$L_{cw} = L_c - \frac{M^2}{L_w} \quad (7)$$

$$K = \sqrt{1 - \frac{L_{cw}}{L_c}} \quad (8)$$

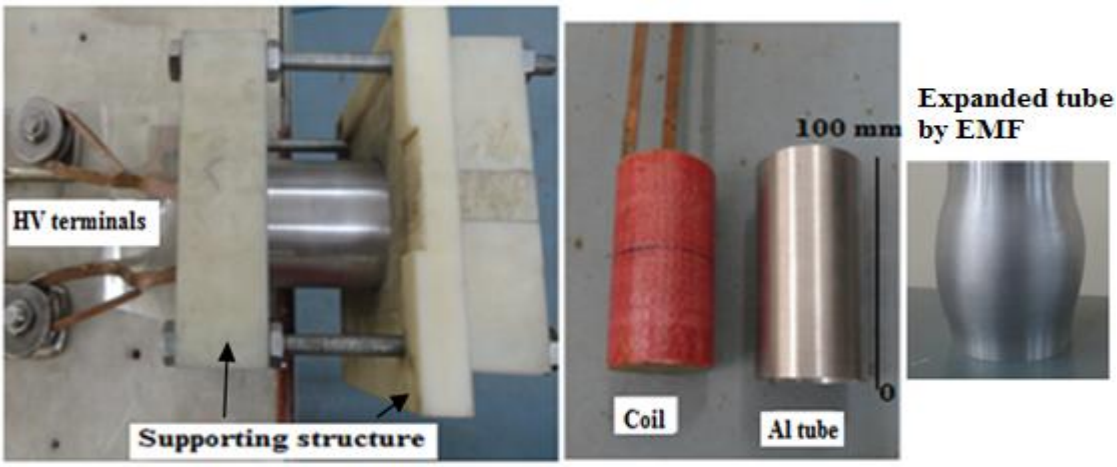

Figure 4: *Experimental set up and expanded tube*

3 Numerical simulation

A 2D axisymmetric numerical simulation model is developed in COMSOL multiphysics. In the electromagnetic module, the coil is excited by under damped current and the generated Lorentz force is communicated to structural mechanics model sequentially at each time step. Moving mesh is used to avoid the mesh distortion at large displacement. Structural mechanics module use Eq. 9 to give tube deformation under the acting Lorentz force.

$$\rho \frac{d^2\overline{u}}{dt^2} - \Delta \cdot \sigma_s = \overline{f_m} \tag{9}$$

Here, ρ is the tube density, u is the displacement vector, σ_s is stress tensor and f_m is the magnetic force density. For tube flow stress, Johnson-Cook plasticity model as given by Eq.10 is used.

$$\sigma = [A + B(\varepsilon)^n][1 + C\ ln\ (\dot{\varepsilon})] \tag{10}$$

Where σ denotes the effective Von Misses stress, ε is effective plastic strain, $\dot{\varepsilon}$ is strain rate and A, B, n, C are the material constitutive parameters (Doley and Kore, 2014). Temperature effect on material behavior is not considered here as small rise in temperature has little influence on electrical and mechanical properties of workpiece material (Haratmeh et al., 2017). For boundary condition, the coil is fixed and only tube is free to move under generated magnetic force. Tube ends are not fixed as radial deformation of the tube results in reduction of tube length axially. Initially, only the magnetic field study is performed to obtain the coupling factor for different tube diameters. When the helical coil is excited by current, by law of electromagnetic induction, eddy current is induced in the

tube having the direction opposite to that of coil current. Similar to transformer, current in the tube will be number of turns times coil current for ideal coupling factor K=1. In numerical simulation, K can be determined by comparing coil and tube current magnitude as given in Eq. 11.

$$K = \frac{I_w}{NI_c} \tag{11}$$

Where I_w is the eddy current flowing through the tube, N is the number of turns of tool coil and I_c is the current through the coil. A 2D axisymmetric COMSOL model with meshing and tube surface displacement is shown in Fig. 5.

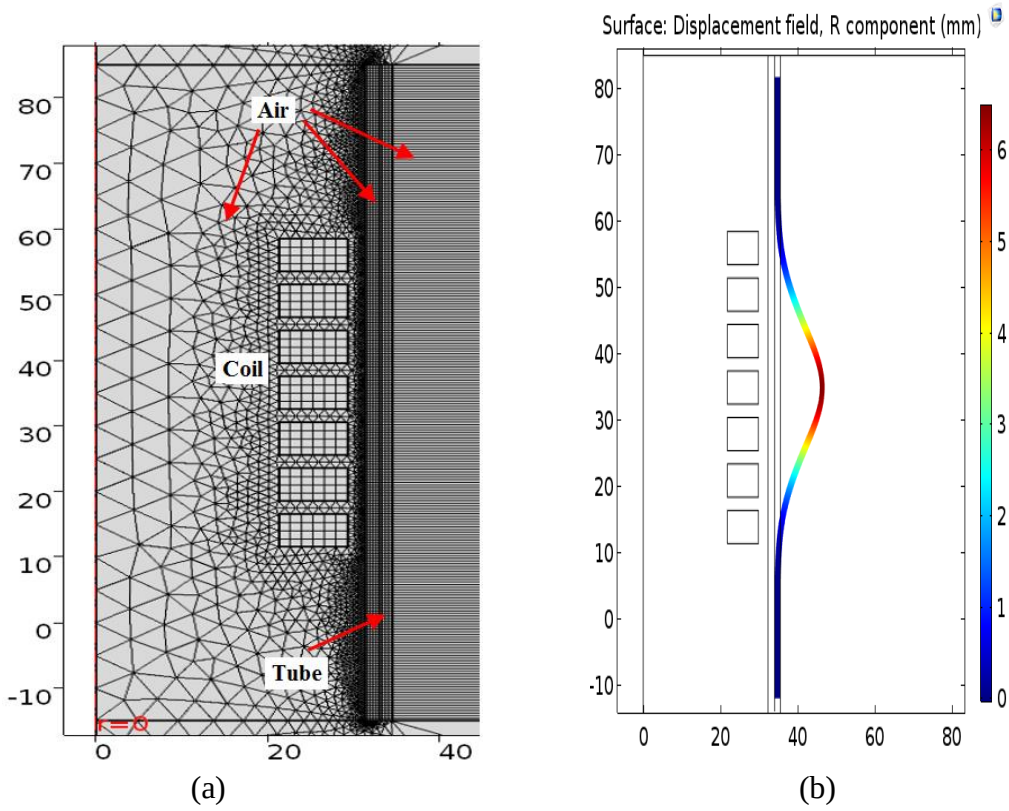

Figure 5: *COMSOL 2D (a) meshing and (b) tube displacement surface plot*

4 Results and discussion

Table 1 shows the measured experimental parameters. System resistance R_s and inductance L_s are constant and their values are 8.8 mΩ and 0.7 µH respectively. With the increase in the distance 'h' between coil and workpiece, inductance L_{cw} increased and resistance R_{cw} decreased as in accordance with Eq. 1 and 2. R_{cw} is coupled resistance of the coil with workpiece and β is the current damping coefficient.

h (mm)	L_{cw} (μH)	R_{cw} (mΩ)	β (1/sec)	I_{peak} (kA)
3	0.831	5.97	3592	105.8
4	0.953	5.61	2943	103.6
5	1.046	5.43	2595	101.9
6	1.120	5.12	2285	101.1

Table 1: *Discharge circuit parameters under different h*

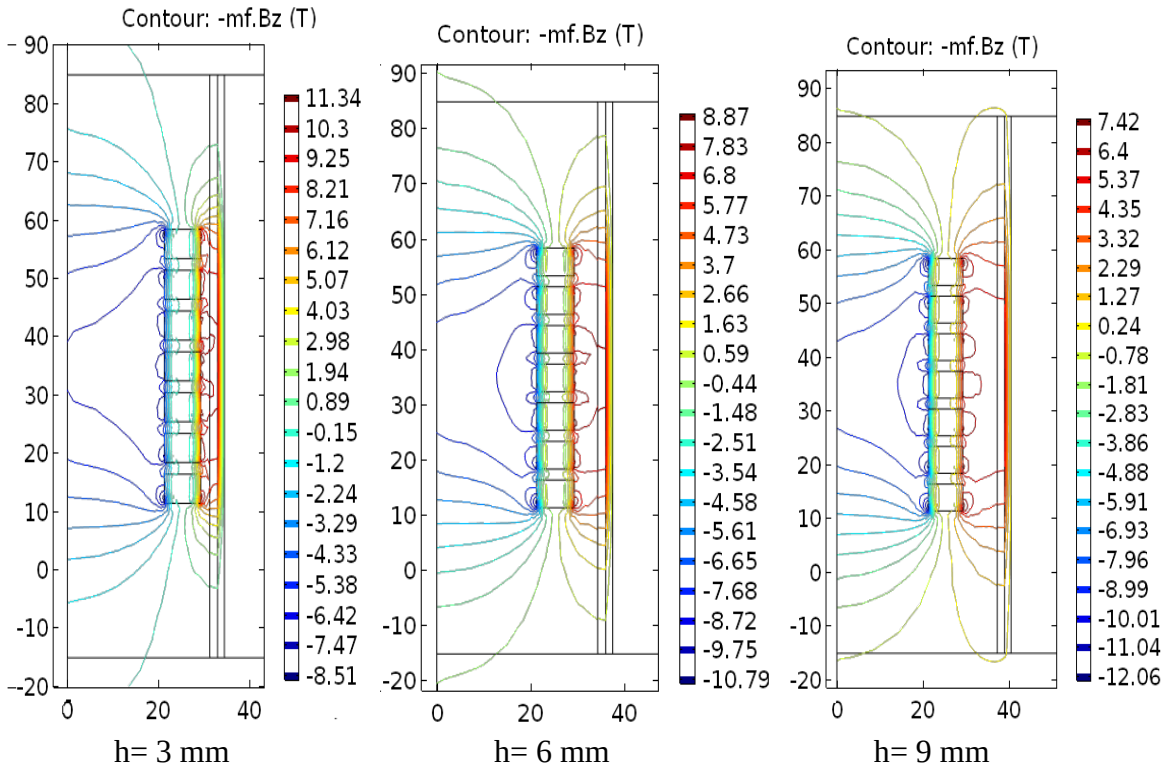

Figure 6: *Coil- tube magnetic flux linkage for different h*

When the skin depth is small compared to work piece thickness, magnetic pressure acting on the workpiece is proportional to square of magnetic flux density present in the coil-workpiece gap [Psyk et al., 2011]. Fig 6 shows the axial magnetic contour plot. Out of the total magnetic flux produced by the coil, some flux lines are not linked with the workpiece known as leakage flux. It can be observed from Fig. 6 that lesser the gap between the coil and the tube, more flux is linked with the tube. This causes improvement in the coil-tube magnetic coupling and magnetic pressure acting on the tube.

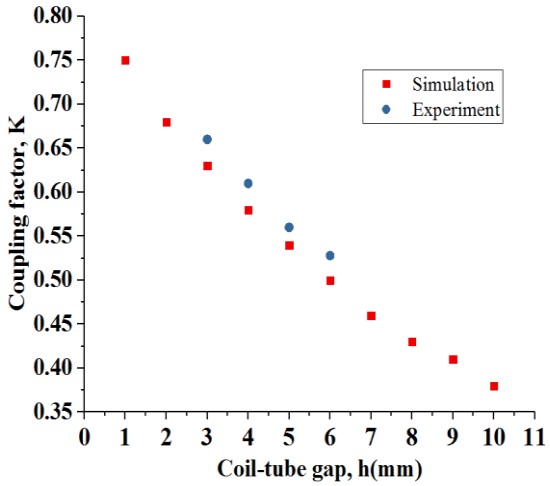

Figure 7: *Coupling factor variation with h*

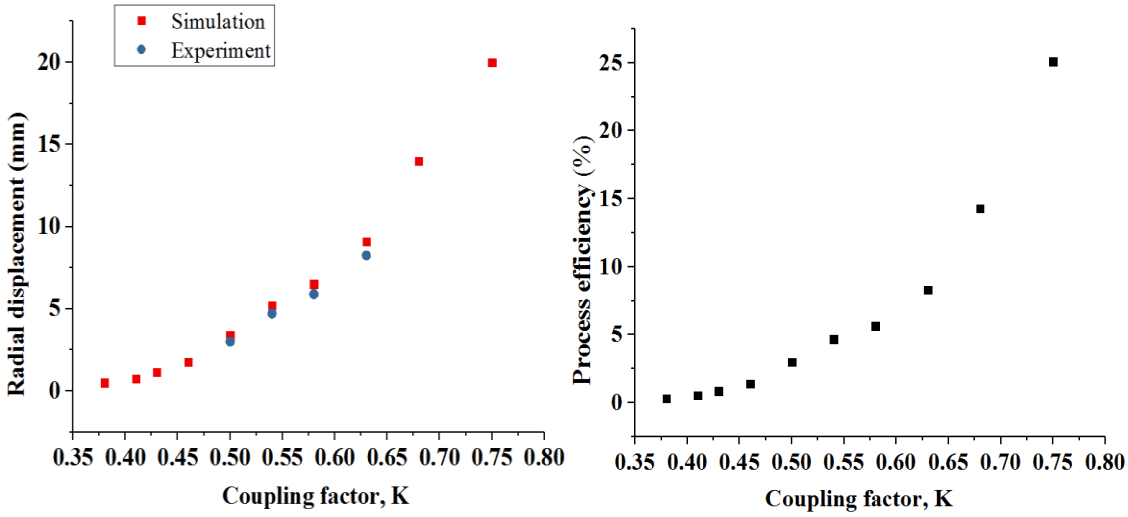

(a) (b)

Figure 8: *Variation of (a) tube displacement and (b) forming efficiency with coupling factor*

Fig. 7 shows the variation of coupling factor K with the coil-tube gap (h). Experimentally obtained K (Eq.8) is compared with numerical one (Eq. 11). Decrease in K is observed with increase in h. Fig. 8 depicts the tube radial displacement and the EMF process efficiency change with K variation. Tube displacement is measured at maximum forming point of the tube whereas process efficiency is obtained from the ratio of plastic deformation energy of the tube to the stored energy in the capacitor. Experimentally obtained results show good agreement with simulation results. It can be seen that the radial displacement of tube and process efficiency follow a smooth exponential type curve that

increases as K increases. The coil-tube magnetic coupling has a significant effect on tube displacement and forming efficiency.

During discharging of capacitive energy into the coil, voltage gets developed between the turns of the coil and between coil and workpiece. While placing the workpiece closer to the coil short circuit and arcing between coupling materials must be avoided. This can be done by providing insulation over the coil which has sufficient electric and thermal strength.

6 Conclusion

Electromagnetic forming experiments and simulations are carried out on aluminium 5052 tubular workpieces. The tool coil and tubular workpiece magnetic coupling is varied by varying the gap between them and the effect of coupling variation on tube displacement and process efficiency is observed. Numerical simulated results which are well agreed with experimental observation showed that the process efficiency and the tube displacement increase exponentially with the increment in coil-tube magnetic coupling factor. Thus positioning of the coil and the workpiece is an important aspect in designing the electromagnetic forming set up.

Acknowledgments

We would like to express our gratitude to Shri. R. K. Rajawat (Head APPD Division, BARC) for his constant encouragement and support.

References

Doley, J., Kore, S., 2014. FEM Study on Electromagnetic Formability of AZ31B Magnesium alloy. Proceedings of the 6th International Conference on High Speed Forming, Korea, pp. 273-280.

Golovashchenko, S., 2006. Electromagnetic forming and joining for automotive applications. Proceedings of the 2nd International Conference on High Speed Forming, Dortmund, Germany, pp. 201-206.

Haratmeh, H. E., Arezoodar, A. F., Farzin, M., 2017. Numerical and experimental investigation of inward tube electromagnetic forming. The International Journal of Advanced Manufacturing Technology 88 (5-8), pp. 1175–1185.

Haiping, Y., Chunfeng, L., 2009. Effects of current frequency on electromagnetic tube compression. Journal of Materials Processing Technology 209 (2), pp. 1053-1059.

Mamalis, A. G., Manolakos, D. E., Kladas, A. G., Koumoutsos, A. K., 2004. Electromagnetic forming and powder processing: Trends and developments. Applied Mechanics Reviews, 57 (4), pp. 299-324.

Psyk, V., Risch, D., Kinsey, B.L., Tekkaya, A.E., Kleiner, M., 2011. Electromagnetic forming – A review. Journal of Materials Processing Technology 211 (5), pp. 787-829.

Xu, W., Fang, H., Xu, W., 2008. Analysis of the variation regularity of the parameters of the discharge circuit with the distance between workpiece and inductor for electromagnetic forming processes. Journal of Materials Processing Technology 203 (1-3), pp. 216–220.

Zapata, J. R. A., Bay, F., 2016. Modeling and Analysis of Electromagnetism in Magnetic Forming Processes. IEEE Transactions on Magnetics 52 (5), Article Sequence Number: 7004011.